RSC Advances

PAPER

View Article Online
View Journal | View Issue

Cite this: *RSC Adv.*, 2017, **7**, 5621

MIL-100(Fe)-catalyzed efficient conversion of hexoses to lactic acid†

Shan Huang, Kai-Li Yang, Xiao-Fang Liu, Hu Pan, Heng Zhang and Song Yang*

Received 8th November 2016
Accepted 27th December 2016

DOI: 10.1039/c6ra26469g

www.rsc.org/advances

MIL-100(Fe) was used for the first time in the catalytic transformation of hexose sugars into lactic acid (LA). The as-synthesized MIL-100(Fe) was systematically characterized, and its superior morphological and textural properties were demonstrated to contribute greatly to the pronounced catalytic performance in fructose-to-LA conversion (up to 32% yield), as compared with other catalysts like Cu-BTC and MIL-100(Cr). The effects of reaction conditions including temperature, reaction time, and substrate loading were explored. In addition, MIL-100(Fe) could be easily reused for 4 cycles with no evident decrease in catalytic activity.

1. Introduction

Lignocellulosic biomass is considered to be a replacement for fossil energy, and efficient catalytic conversions of renewable lignocellulosic biomass to produce high value-added chemicals and biofuels are a potential way to mitigate the rigorously deteriorating pollution of the environment, the consumption of fossil fuels and the attendant global warming.[1–5] As a precursor to produce biodegradable polylactic acid (PLA), LA, a high-potential versatile biobased platform molecule, has been widely employed in the food industry as well as the cosmetic industry. It is also a remarkable molecule for the synthesis of a wide range of attractive intermediates such as acrylic acid, propylene glycol, 2,3-pentanedione, acetaldehyde, pyruvic acid, 1,2-propanediol and lactic acid esters.[6] The annual demand for LA is expected to increase to 6×10^5 tons by 2020.[7]

LA is generally produced *via* conventional fermentation of carbohydrates.[8] Nevertheless, this process suffers from low space-time yields, and complicated and tedious separation process with significant amounts of salt wastes formed. Therefore, alternative chemo-catalytic approaches toward LA and alkyl lactates from renewable carbohydrates are of great interest.[9–13] Lewis acids were demonstrated to play an extremely essential role in retro-aldol reaction, isomerization and 1,2-hydride shift for the whole catalytic production of LA from sugars.[11] For instance, Holm *et al.* found that Lewis acidic zeotype materials Sn-Beta exhibited good activity in the conversion of mono- and disaccharides to methyl lactate (MLA) and LA at 160 °C within 20 h, and acceptable amounts of LA (28% for sucrose and 27% for fructose) were formed in H_2O by using sucrose and fructose as substrate.[11] Chambon *et al.* employed Lewis acidic tungstated alumina (AlW) to catalyze cellulose into LA with 27% yield at 190 °C for 24 h, and a moderate LA yield of 21% could be obtained from glucose at 190 °C for 1 h.[12] However, these solid catalysts are generally not active enough for producing LA from sugars. Therefore, research on the design and use of efficient Lewis acid catalysts in selective transformation of hexose into LA is highly desirable.

In virtue of the conspicuous advantages of large surface area, extra-high porosity, adjustable pore size, structural diversity, high thermal and chemical stability, and controllable composition with lots of coordinatively unsaturated metal sites (CUS), metal–organic frameworks (MOFs) has attracted increasing attention and been applied in various fields such as imaging,[14] sensors,[15] adsorption,[16] separation,[17] gas storage,[18] drug carrier,[19] and heterogeneous catalysis.[20–22] Among the Lewis acidic metal–organic framework materials (*e.g.*, chromium,[23] copper,[24] and zirconium carboxylates[25]), MIL-100(Fe) is an attractive candidate in view that the precursor material, iron, is much more abundant, cheap, nonhazardous and easy to get, and that the quality and structure properties of MIL-100(Fe) are spectacular and simple to prepare.[26] The three-dimensional crystalline iron(III) trimesate MIL-100(Fe) possesses two different sets of mesoporous cages (25 Å and 29 Å in diameter) with microporous windows (5.5 Å and 8.6 Å in diameter), which is build up from trimers of iron octahedral sharing a common vertex μ_3-O linked by the benzene-1,3,5-trimesic acid.[26,28] The Lewis acid sites are generated by removing the OH^- or F^- anions that coordinated with the iron octahedral.[27,34] In recent years, MIL-100(Fe) has been used as a Lewis acid catalyst to show outstanding performance in organic synthesis.[28–33]

State Key Laboratory Breeding Base of Green Pesticide & Agricultural Bioengineering, Key Laboratory of Green Pesticide & Agricultural Bioengineering, Ministry of Education, State-Local Joint Laboratory for Comprehensive Utilization of Biomass, Center for Research & Development of Fine Chemicals, Guizhou University, Guiyang 550025, China. E-mail: jhzx.msm@gmail.com; Fax: +86-851-8829-2170; Tel: +86-851-8829-2171

† Electronic supplementary information (ESI) available. See DOI: 10.1039/c6ra26469g

To the best of our knowledge, rare study has been conducted on the synthesis of LA from hexose catalyzed by MOFs. Herein, we examined the catalytic performance of MIL-100(Fe), Cu-BTC and MIL-100(Cr) in the direct conversion of fructose to LA in H_2O.

2. Experimental

2.1 Materials

All the reagents were used as received without any further purification. Fructose (99%), D(+)-glucose (AR), sucrose (AR), D-(+)-cellobiose (98%), inulin, LA (99%), formic acid (FA), (HPLC $\geq$ 98%), 5-hydroxymethylfurfural (HMF; 99%), CrO_3 (99%, AR), $Cu(NO_3)_2 \cdot 3H_2O$ (99%, AR), $Fe(NO_3)_3 \cdot 9H_2O$ (AR), iron powder (98%), and hydrofluoric acid (49% in water) were purchased from Shanghai Aladdin Industrial Inc. 1,3,5-Benzenetricarboxylic acid (H_3BTC), methyl lactate (MLA; 98%), acetic acid (AA; 99.8%) and levulinic acid (LeA; 99%) were purchased from J & K Scientific Ltd. Nitric acid (65%) and ethanol (AR grade) were purchased from Chongqing Chuandong Chemical co., Ltd. Deionized water was from Milli-Q Advantage A10 (USA) ultrapure water purification system.

2.2 Analysis

LA, FA and AA were analyzed *via* an Agilent 1100 HPLC using an Agilent TC-C18 column (4.6 mm ID $\times$ 250 mm) with 0.05 wt% H_3PO_4 aqueous solution (A) and methanol (B) ($V_A : V_B = 90 : 10$) as eluent. The UV detector was set at a wavelength of 210 nm, the columns were thermostatized at 30 °C and the flow rate was set at 0.6 mL min^{-1}. For the detection of LeA, the mobile phase was consisted of 0.05 wt% H_3PO_4 aqueous solution (C) and acetonitrile (D) ($V_C : V_D = 90 : 10$). The UV detector was set at a wavelength of 254 nm, the columns were thermostatized at 30 °C and the flow rate was set at 0.6 mL min^{-1}. For the detection of HMF, the mobile phase was consisted of methanol (E) and H_2O (F) ($V_E/V_F = 65 : 35$) at a flow rate of 1.0 mL min^{-1}. The UV detector was set at a wavelength of 280 nm. For the HPLC analyses, 0.5 mL of the reaction mixture was diluted to a total volume of 5.0 mL with the eluent. The products were identified by UV (210 nm) detectors by comparing them to the original samples. Sugars were analyzed by Agilent 1100 HPLC fitted with an Aminex HPX-87H column (Bio-Rad, Richmond, CA) and a refractive index (RI) detector with the mobile phase CH_3CN (G) and H_2O (H) ($V_G/V_H = 80 : 20$) at a flow rate of 1.0 mL min^{-1}.

The conversion of sugar and LA yield were calculated according to eqn (1) and (2), respectively.

$$X\,(\text{sugar conversion, \%}) = (\text{mass of sugar converted/ mass of starting sugar}) \times 100\% \quad (1)$$

$$Y\,(\text{product yield, \%}) = (\text{mole of carbon in product/ mole of carbon in sugar}) \times 100\% \quad (2)$$

2.3 Catalyst preparation and characterization

MIL-100(Fe) was synthesized hydrothermally by reacting of iron powder with H_3BTC in the presence of hydrofluoric acid, nitric acid and H_2O with the composition of 1.0 Fe^0 : 0.67 1,3,5-BTC : 2.0 HF : 0.6 HNO_3 : 277 H_2O at 150 °C for 12 h according to the literature.[34] Cu-BTC and MIL-100(Cr) were hydrothermally synthesized following the procedure described in the previous literatures (see catalyst preparation and characterization in ESI†).[35,36]

The X-ray powder diffraction (XRD) patterns were obtained on a XPD-6000 diffractometer using CuKα radiation ($k = 0.1541$ nm) in a scanning range of 5–35° at a scanning rate of 1° min^{-1}. The scanning electron microscope (SEM) observations were performed on a ZEISS apparatus equipped with a field emission gun. The measurements of N_2 adsorption were performed on a Micromeritics ASAP 2020 apparatus at −196 °C, prior to the adsorption measurement, the sample was outgassed in vacuum at 150 °C for 12 h. The specific surface areas of the investigated samples were calculated using the multiple-point Brunauer–Emmett–Teller (BET) method in the relative pressure range of $p/p_0 = 0.05$–0.20 and the total pore volumes were determined at a relative pressure of 0.95. The pore size distribution curves were determined from the adsorption isotherms by the Density Functional Theory (DFT) method. The thermogravimetric analysis (TGA) was performed on a NETZSCH STA 449 C instrument from 35 to 600 °C, using a heating rate of 10 °C min^{-1} under a N_2 flow (40 mL min^{-1}). The FT-IR spectra were collected on a Nicolet 360 Fourier transform IR spectrophotometer in KBr disks at room temperature. The acid properties of MIL-100(Fe) and other two MOFs were characterized by using pyridine adsorption infrared spectroscopy recorded on Brooke Tensor 27 Fourier infrared spectrometer. The sample was activated at 150 °C for 3 h and then pressed into circular uniform slices (15 mm diameter, 15 mg) in the self-supported disk (without KBr) under the infrared lamp light with 12 KPa pressure. The spectrum was recorded as background after cooling the tablet down to room temperature. Pyridine vapour was then introduced into the cell. The amount of iron leaching was determined by ICP-MS on a Vista Axial instrument (Varian of USA).

2.4 Catalytic reactions

All experiments were carried out in a 25 mL Teflon lined autoclave. For the conversion of sugar to LA, substrate (50 mg) catalyst (50 mg) and 10 mL H_2O were added into the reactor, which was then placed into a preheated oil bath with magnetic stirring at 190 °C for 2 h. The reactor was all immersed in the oil bath and the reaction time was started to record immediately. After the reaction finished, the reactor was fast took out and cooled rapidly by tap-water. Afterward, the catalyst was recovered through centrifugation and the reaction liquid was filtered with a 0.45 μm syringe filter, and then analyzed by HPLC.

For the sake of comparison, blank experiment without catalyst and experiments with metal salt, $Fe(NO_3)_3 \cdot 9H_2O$, and two Lewis acid MOFs materials (*i.e.*, Cu-BTC and MIL-100(Cr)) were carried out. A number of recycling experiments were also conducted to examine the catalyst stability. After each run, the recovered solid was washed with ethanol to remove the adsorbed organic species.

3. Results and discussion

3.1 Catalyst characterization

The experimental XRD pattern of MIL-100(Fe) is illustrated in Fig. 1. Correspondingly, the XRD patterns of MIL-100(Cr) and Cu-BTC are displayed in Fig. S2.† It can be seen that the XRD pattern of the prepared catalyst is in good agreement with the simulated one, showing the successful preparation of MOFs.

The textural property of the synthesized MIL-100(Fe) assessed by N_2 adsorption isotherm is presented in Fig. 2. The prepared MIL-100(Fe) gave a BET surface area of 1650 $m^2\ g^{-1}$ with a pore volume of 0.74 $cm^3\ g^{-1}$, and the pore size distribution of MIL-100(Fe) estimated by using the DFT method displayed two different pore sizes (about 1.9 and 2.2 nm, respectively; Fig. S1†), suggesting that there are two types of cages in the framework of MIL-100(Fe).

Fig. 3 reveals that the MIL-100(Fe) is stable up to 330 °C, as verified by TG analysis, and there are three weight loss processes between 35 and 600 °C. The first one (about 4 wt%) ranging from 35 to 100 °C is attributed to the desorption of free water molecules inside the pores. The second weight loss (about 8 wt%) in the range of 100–330 °C is water coordinated to the iron trimers. The final weight loss, between 330 and 530 °C (about 41 wt%), is related to the decomposition of the H_3BTC. Similar TG curves of both MIL-100(Cr) and Cu-BTC are obtained with MIL-100(Fe), MIL-100(Cr) is stable up to 300 °C and Cu-BTC is 250 °C, respectively.

Fig. 4 shows the SEM image of MIL-100(Fe). The synthesized MIL-100(Fe) is mainly octahedral in shape, and the particle is

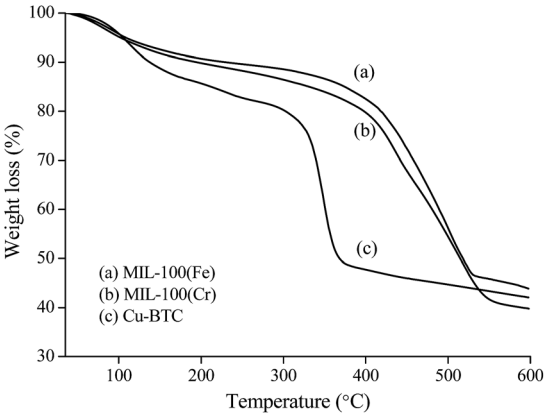

Fig. 3 TG curves of the synthesized MIL-100(Fe), MIL-100(Cr) and Cu-BTC.

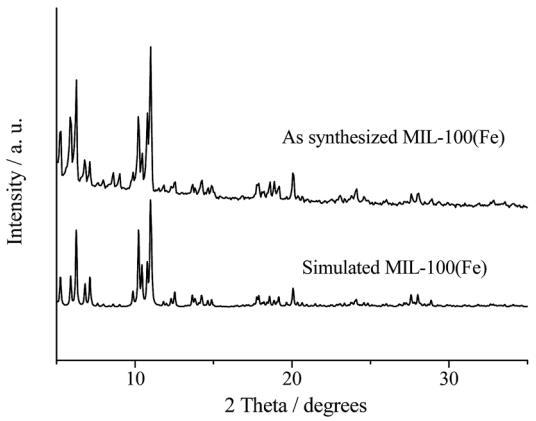

Fig. 1 XRD patterns of synthesized and simulated MIL-100(Fe).

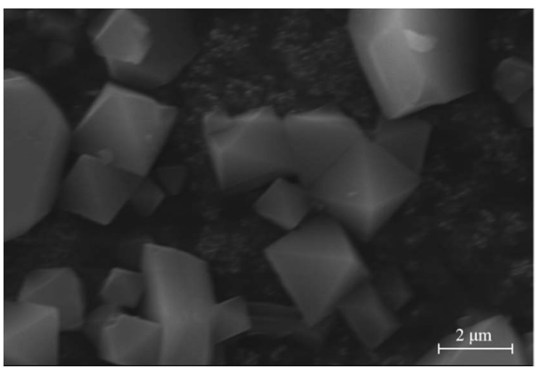

Fig. 4 SEM image of the synthesized MIL-100(Fe).

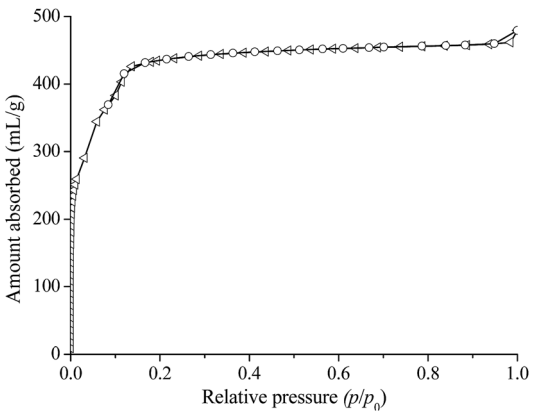

Fig. 2 N_2 isotherm of the synthesized MIL-100(Fe).

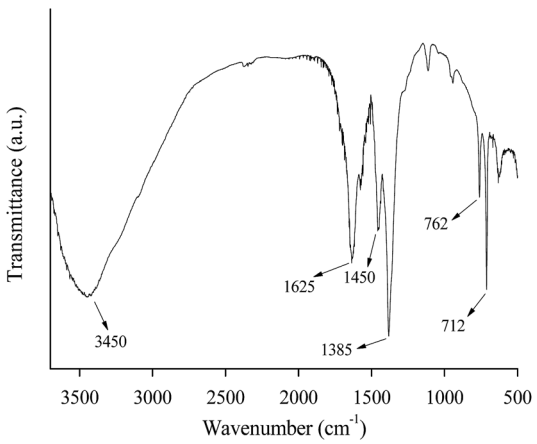

Fig. 5 FT-IR spectrum of the synthesized MIL-100(Fe).

uniform in size. Fig. 5 indicates the FT-IR spectrum of the synthesized MIL-100(Fe). The band at 3445 cm^{-1} was attributed to –OH, 1385, 1450 and 1625 cm^{-1} were ν(C–O) stretching vibration, ν(–OH) flexural vibration and ν(C=O) stretching vibration, and 762 and 712 cm^{-1} were fingerprints assigned to ν(C–H) stretching vibration of benzene ring, respectively. There is no peak at 1710–1720 cm^{-1} assigned to the C=O stretching vibration of H_3BTC, indicating that the purification procedure used here is particularly effective to remove residual H_3BTC. On the basis of the characterization results above (*i.e.*, XRD, N_2 adsorption, TGA, SEM and FT-IR), it can be concluded that MIL-100(Fe) is successfully synthesized in this work.

3.2 Catalytic activity

3.2.1 Transformation of fructose into LA by different catalysts. Catalytic conversion of fructose by using different catalysts was carried out, and the results are shown in Table 1. 3% yield of LA was obtained without a catalyst.[37] Comparison of the blank control trial with the catalytic result of MIL-100(Fe) illustrated that this MOF material showed good activity. In contrast, only about 10% yield of LA was achieved over the homogeneous iron salt, $Fe(NO_3)_3$.

From Table 1, it can be seen that LA, together with HMF, LeA, AA, and FA, is the product in this reaction system. MIL-100(Fe) is the most effective catalyst among the examined Lewis acid materials, giving LA yield of 32%, HMF of 17%, FA of 9%, AA of 7%, and LeA of 6%. The good catalytic results of MIL-100(Fe) could never be existed without its excellent morphological characteristics and textural properties. Fig. 2 shows that MIL-100(Fe) possesses higher specific surface area (S_{BET} = 1650 m^2 g^{-1}) than MIL-100(Cr) (S_{BET} = 1330 m^2 g^{-1})[36] and Cu-BTC (S_{BET} = 1223 m^2 g^{-1}).[35] Besides, the thermal stability is also checked. It can be observed that the thermal stability of MIL-100(Fe) is better than that of other two materials (Fig. 3), which is in agreement with the catalytic results (*i.e.*, 20% LA yield for MIL-100(Cr), and 18% for Cu-BTC).

To figure out the intrinsic reason for the activity sequence of the three MOFs, their acid properties were further compared. The metal cations that are integral to the framework could be made catalytically-active by removal of their solvent ligands to a vacant coordination site as a Lewis acid. In this work, we characterized the acid properties of the three MOFs by using pyridine adsorption infrared spectroscopy. Fig. S4† shows the infrared spectra of pyridine adsorbed on those MOFs. The intensity of the bands between 1000 and 1100 cm^{-1}, which assigned to pyridine molecule chemisorbed on Lewis acid sites of MIL-100(Fe),[38] was much stronger than Cu-BTC and MIL-100(Cr), illustrating that the concentration of Lewis acid centers in MIL-100(Fe) was higher than that of other two materials. Thus, the best performance of the Lewis acid MIL-100(Fe) could be expected.

Table 1 Conversion of fructose into LA catalyzed by various catalysts[a]

			Yield (%)					
Entry	Catalyst	Conv. (%)	LA	HMF	FA	AA	LeA	Total
1	No catalyst	39	3	11	7	2	3	26
2	$Fe(NO_3)_3$	68	10	9	3	16	13	51
3	MIL-100(Fe)	87	32	17	9	7	6	71
4	Cu-BTC	73	18	26	7	3	6	60
5	MIL-100(Cr)	76	20	28	5	5	3	61

[a] Reaction conditions: fructose 0.05 g, catalyst 0.05 g, H_2O 10 mL, 190 °C, 2 h.

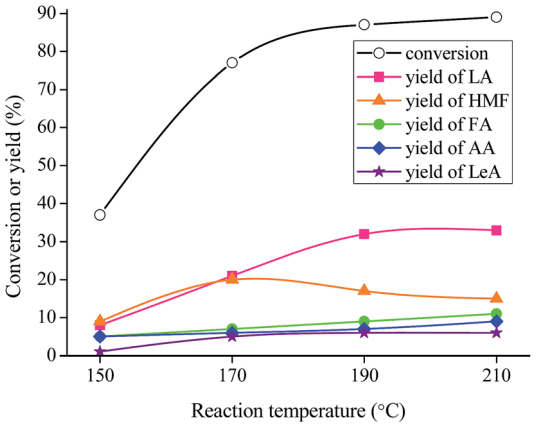

Fig. 6 Influence of reaction temperature on the yield of LA. Reaction conditions: fructose 0.05 g, MIL-100(Fe) 0.05 g, water 10 mL, 2 h.

3.2.2 Influence of reaction temperature on the production of LA. In subsequent tests, fructose was used as substrate with MIL-100(Fe) as catalyst. Reaction temperature was an important factor (Fig. 6). When the reaction temperature was increased from 150 to 210 °C, the conversion of fructose was improved sharply from 37% to 89%. The yield of LA increased with the extension of reaction temperature and reached the highest yield (33%) at 210 °C, while the yields of FA, LeA and AA were as well increased with increasing temperature. Because the yield of LA did not increase markedly above 190 °C (32%), the reaction temperature was fixed at 190 °C in the following study.

3.2.3 Effect of reaction time on the conversion of fructose to LA. The effect of reaction time on production of LA from fructose was further explored (Fig. 7). The results show that prolonging the reaction time from 0.5 to 2 h, MIL-100(Fe) could give 14% and 32% yields of LA at 70% and 87% conversion, respectively. When further extending the time to 3.5 h and 5 h, no increase in LA yield was observed but a slight increase of fructose conversion, suggesting that by-products were formed more and more. Thus, 2 h was selected as the optimal time for the catalytic reaction.

3.2.4 Results of different fructose amount on the production of LA. Fig. 8 showed that the optimum amount of fructose was 0.05 g, further increasing the amount of fructose from 0.05 to 0.2 g, the yield of LA only decreased slightly. By that data, we could conclude that MIL-100(Fe) used in this reaction maintained active at high concentrations of fructose. Hence, the initial substrate amount was fixed at 0.05 g.

3.2.5 Conversions of different sugars into LA catalyzed by MIL-100(Fe). The hydrothermal conversions of different sugars

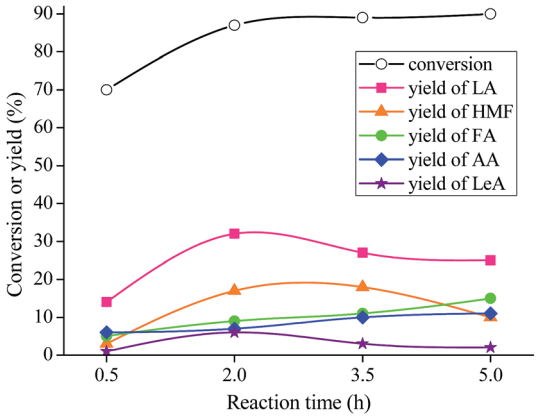

Fig. 7 Influence of reaction time on the yield of LA. Reaction conditions: fructose 0.05 g, MIL-100(Fe) 0.05 g, water 10 mL, 190 °C.

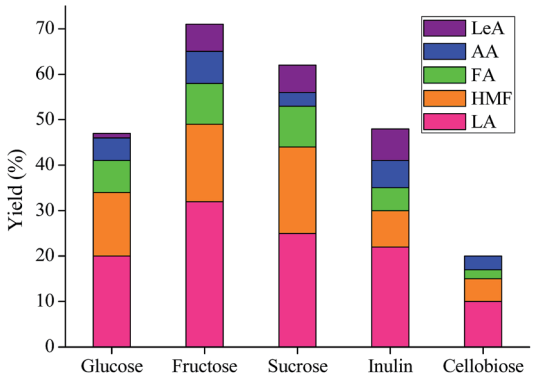

Fig. 9 Conversion of different substrates using MIL-100(Fe) as a catalyst. Reaction conditions: substrate 0.05 g, catalyst 0.05 g, H_2O 10 mL, 190 °C, 2 h.

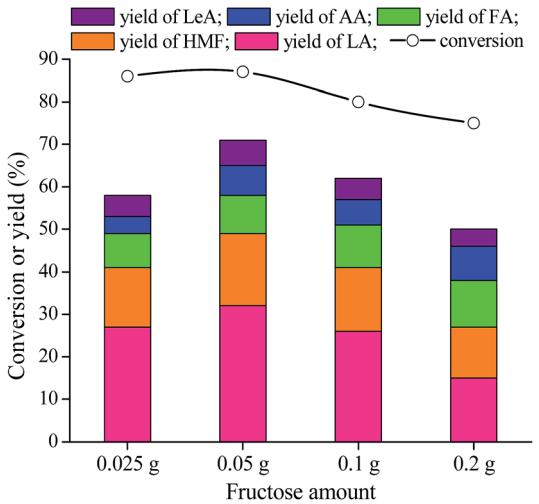

Fig. 8 Conversion of fructose into LA with different initial amount of fructose. Reaction conditions: MIL-100(Fe) 0.05 g, water 10 mL, 190 °C, 2 h.

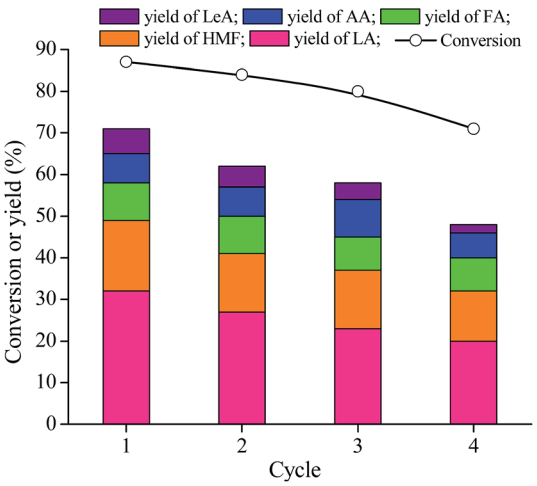

Fig. 10 Reusability of MIL-100(Fe) for the conversion of fructose to LA. Reaction conditions: fructose 0.05 g, MIL-100(Fe) 0.05 g, water 10 mL, 190 °C, 2 h.

were also investigated by using MIL-100(Fe) as catalyst. It is easy to form HMF and LeA from fructose catalyzed by Brønsted acids,[39,40] while Lewis acids are demonstrated to catalyze retro-aldol reaction, isomerization and 1,2-hydride shift for fructose being converted to lactic acid.[11] The results presented in Fig. 9 show that there is 20% yield of LA with glucose as substrate, and the yields of HMF and LeA are less than LA, which further proved the view above. When using disaccharide (*e.g.*, sucrose and cellobiose) and polysaccharide (*e.g.*, inulin) as substrate, a LA yield of 25%, 10% and 22% was achieved, respectively. In addition, changing the solvent from water to methanol led to the formation of MLA (Table S1†). For fructose, a 33% yield of MLA were obtained (entry 4).

3.3 Reuse of catalyst

The reusability of catalyst in the hydrothermal conversion of fructose was also evaluated (Fig. 10). In a forth-cycle experiment, the catalyst was separated by simple centrifugation followed by washing with ethanol to remove adsorbed compounds and then dried at 80 °C before the next cycle. There was still 20% yield of LA when the MIL-100(Fe) was reused four times. The general causes of the apparent catalyst deactivation fall into two respects. Firstly, the accelerated deposition of some oligomeric products in pores that resulted in the blocking of the active sites and partial structural changes within the catalyst.[21] To verify this, the recovered catalyst was characterized by N_2 adsorption–desorption, XRD, and FT-IR. As shown in Fig. S5 and S6,† it can be seen that the XRD pattern and FT-IR spectra of the used catalyst did not show remarkably changes compared to the fresh MIL-100(Fe), illustrating that the framework structure of this MOF material was maintained. From Fig. S7,† there was a reduction of the BET surface area and pore volume, which might hinder the mass transport for producing LA. Secondly, a small quantity of active sites were leached out from the reused catalyst (after it being used 4 times). We found some H_3BTC in the filtrate (of the fourth cycle) by HPLC, explaining that the catalyst released gradually trimesic acid. And the loss of the

original metal–organic linker bond could lead to leaching of some metal ion from the MOF.[41] ICP-MS analysis showed the presence of 3.03 ppm of Fe in the filtrate of the fourth cycle, which means that the reused catalyst released some iron. These two changes led to a slight decrease in acidity density of catalyst, which further resulted in lower selectivity to LA. Besides, from the result of NH_3-TPD in Fig. S8,† the acidity of the recovered catalyst decreased slightly, which also led to lower selectivity toward lactic acid. In order to better reuse the catalyst, we further employed a simple method for regeneration of the recovered catalyst, referring to a protocol reported by Han *et al.* (see ESI†).[42] Activity evaluation revealed that the regenerated MIL-100(Fe) regained the catalytic activity (28% yield of LA). Even though this catalyst couldn't keep completely stable, it still made MIL-100(Fe) an alternative catalyst for the conversion of fructose to LA.

4. Conclusions

In summary, the as-synthesized MIL-100(Fe) was used for the first time as Lewis acid catalyst for catalytic transformation of sugars to LA, and showed satisfactory performance. A high yield of LA, up to 32%, was produced from fructose with MIL-100(Fe) in H_2O at 190 °C for 2 h. In order to better understand the relationship between the structure properties and the catalytic performance, the catalytic activities of Cu-BTC and MIL-100(Cr) were also tested and compared. The results showed that both materials are not as active as MIL-100(Fe). The metal nature in the framework, specific surface area, stability and Lewis acid properties of these MOFs were demonstrated to influence their catalytic activities. Furthermore, the MIL-100(Fe) could be easily reused for 4 cycles. Therefore, MOFs are very promising materials for biomass conversion, especially for LA production.

Acknowledgements

This work was financially supported by the National Natural Science Foundation of China (No. 21576059 & 21666008), the Key Technologies R & D Program (No. 2014BAD23B01), and the Innovation Fund for Graduate Students of Guizhou University (No. 2016075).

References

1 K. Yan, G. S. Wu, T. Lafleur and C. Jarvis, *Renewable Sustainable Energy Rev.*, 2014, **38**, 663.
2 K. Yan, C. Jarvis, J. Gu and Y. Yan, *Renewable Sustainable Energy Rev.*, 2015, **51**, 986.
3 C. Zhao, T. Brück and J. A. Lercher, *Green Chem.*, 2013, **15**, 1720.
4 H. Li, P. S. Bhadury, A. Riisager and S. Yang, *Catal. Sci. Technol.*, 2014, **4**, 4138.
5 H. Li, Z. Fang and S. Yang, *ChemPlusChem*, 2016, **81**, 135.
6 P. Gallezot, *Chem. Soc. Rev.*, 2012, **41**, 1538.
7 M. Dusselier, P. Van Wouwe, A. Dewaele, E. Makshina and B. F. Sels, *Energy Environ. Sci.*, 2013, **6**, 1415.
8 F. de Clippel, M. Dusselier, R. Van Rompaey, P. Vanelderen, J. Dijkmans, E. Makshina, L. Giebeler, S. Oswald, G. V. Baron, J. F. M. Denayer, P. P. Pescarmona, P. A. Jacobs and B. F. Sels, *J. Am. Chem. Soc.*, 2012, **134**, 10089.
9 Q. Guo, F. T. Fan, E. A. Pidko, W. N. P. van der Graaff, Z. C. Feng, C. Li and E. J. M. Hensen, *ChemSusChem*, 2013, **6**, 1352.
10 F. F. Wang, C. L. Liu and W. S. Dong, *Green Chem.*, 2013, **15**, 2091.
11 M. S. Holm, S. Saravanamurugan and E. Taarning, *Science*, 2010, **328**, 602.
12 F. Chambon, F. Rataboul, C. Pinel, A. Cabiac, E. Guillon and N. Essayem, *Appl. Catal., B*, 2011, **105**, 171.
13 L. S. Yang, X. K. Yang, E. Tian, V. Vattipalli, W. Fan and H. F. Lin, *J. Catal.*, 2016, **333**, 207.
14 K. M. L. Taylor-Pashow, J. D. Rocca, Z. G. Xie, S. Tran and W. B. Lin, *J. Am. Chem. Soc.*, 2009, **131**, 14261.
15 Y. Q. Xiao, Y. J. Cui, Q. Zheng, S. C. Xiang, G. D. Qian and B. L. Chen, *Chem. Commun.*, 2010, **46**, 5503.
16 A. Zukal, M. Opanasenko, M. Rubeš, P. Nachtigall and J. Jagiello, *Catal. Today*, 2015, **243**, 69.
17 S. L. Qiu, M. Xue and G. S. Zhu, *Chem. Soc. Rev.*, 2014, **43**, 6116.
18 J. A. Mason, M. Veenstra and J. R. Long, *Chem. Sci.*, 2014, **5**, 32.
19 S. Rojas, F. J. Carmona, C. R. Maldonado, E. Barea and J. A. R. Navarro, *New J. Chem.*, 2016, **40**, 5690.
20 A. Corma, H. García and F. X. L. i Xamena, *Chem. Rev.*, 2010, **110**, 4606.
21 X. F. Liu, H. Li, H. Zhang, H. Pan, S. Huang, K. L. Yang and S. Yang, *RSC Adv.*, 2016, **6**, 90232.
22 A. Herbst and C. Janiak, *New J. Chem.*, 2016, **40**, 7958.
23 L. Mitchell, B. Gonzalez-Santiago, J. P. S. Mowat, M. E. Gunn, P. Williamson, N. Acerbi, M. L. Clarke and P. A. Wright, *Catal. Sci. Technol.*, 2013, **3**, 606.
24 L. Alaerts, E. Séguin, H. Poelman, F. Thibault-Starzyk, P. A. Jacobs and D. E. De Vos, *Chem.–Eur. J.*, 2006, **12**, 7353.
25 T. L. H. Doan, T. Q. Dao, H. N. Tran, P. H. Tran and T. N. Le, *Dalton Trans.*, 2016, **45**, 7875.
26 L. Mitchell, P. Williamson, B. Ehrlichová, A. E. Anderson, V. R. Seymour, S. E. Ashbrook, N. Acerbi, L. M. Daniels, R. I. Walton, M. L. Clarke and P. A. Wright, *Chem.–Eur. J.*, 2014, **20**, 17185.
27 P. Horcajada, S. Surblé, C. Serre, D. Y. Hong, Y. K. Seo, J. S. Chang, J. M. Grenèche, I. Margiolaki and G. Férey, *Chem. Commun.*, 2007, 2820.
28 A. Dhakshinamoorthy, M. Alvaro, Y. K. Hwang, Y. K. Seo, A. Corma and H. Garcia, *Dalton Trans.*, 2011, **40**, 10719.
29 L. Kurfiřtová, Y. K. Seo, Y. K. Hwang, J. S. Chang and J. Čejka, *Catal. Today*, 2012, **179**, 85.
30 A. Dhakshinamoorthy, M. Alvaro, H. Chevreau, P. Horcajada, T. Devic, C. Serre and H. Garcia, *Catal. Sci. Technol.*, 2012, **2**, 324.
31 F. Vermoortele, R. Ameloot, L. Alaerts, R. Matthessen, B. Carlier, E. V. Ramos Fernandez, J. Gascon, F. Kapteijn and D. E. De Vos, *J. Mater. Chem.*, 2012, **22**, 10313.

32 L. Mitchell, P. Williamson, B. Ehrlichová, A. E. Anderson, V. R. Seymour, S. E. Ashbrook, N. Acerbi, L. M. Daniels, R. I. Walton, M. L. Clarke and P. A. Wright, *Chem.–Eur. J.*, 2014, **20**, 17185.
33 F. M. Zhang, J. Shi, Y. Jin, Y. H. Fu, Y. J. Zhong and W. D. Zhu, *Chem. Eng. J.*, 2015, **259**, 183.
34 J. W. Yoon, Y. K. Seo, Y. K. Hwang, J. S. Chang, H. Leclerc, S. Wuttke, P. Bazin, A. Vimont, M. Daturi, E. Bloch, P. L. Llewellyn, C. Serre, P. Horcajada, J. M. Grenèche, A. E. Rodrigues and G. Férey, *Angew. Chem., Int. Ed.*, 2010, **49**, 5949.
35 M. Hartmann, S. Kunz, D. Himsl and O. Tangermann, *Langmuir*, 2008, **24**, 8634.
36 M. Wickenheisser, F. Jeremias, S. K. Henninger and C. Janiak, *Inorg. Chim. Acta*, 2013, **407**, 145.
37 X. Y. Yan, F. M. Jin, K. Tohji, T. Moriya and H. Enomoto, *J. Mater. Sci.*, 2007, **42**, 995.
38 H. Leclerc, A. Vimont, J. C. Lavalley, M. Daturi, A. D. Wiersum, P. L. Llwellyn, P. Horcajada, G. Férey and C. Serre, *Phys. Chem. Chem. Phys.*, 2011, **13**, 11748.
39 V. Choudhary, S. H. Mushrif, C. Ho, A. Anderko, V. Nikolakis, N. S. Marinkovic, A. I. Frenkel, S. I. Sandler and D. G. Vlachos, *J. Am. Chem. Soc.*, 2013, **135**, 3997.
40 Y. J. Pagán-Torres, T. F. Wang, J. M. R. Gallo, B. H. Shanks and J. A. Dumesic, *ACS Catal.*, 2012, **2**, 930.
41 S. Das, D. E. Johnston and S. Das, *CrystEngComm*, 2012, **14**, 6136.
42 S. Han and M. S. Lah, *Cryst. Growth Des.*, 2015, **15**, 5568.